V International Conference on Computational Methods in Marine Engineering
MARINE 2013
B. Brinkmann and P. Wriggers (Eds)

SIMULATION OF MOONPOOL WATER MOTION

HENRI J.L. VAN DER HEIDEN*, PETER VAN DER PLAS*, ARTHUR E.P. VELDMAN*, R. LUPPES* AND ROEL W.C.P. VERSTAPPEN*

*Computational Mechanics and Numerical Mathematics
Institute of Mathematics and Computing Science
University of Groningen
Groningen, 9747 AG
e-mail: h.j.l.van.der.heiden@rug.nl

Key words: Moonpool water motion, Viscous flow modeling, Turbulence

Abstract. The potentially violent free-surface motion of water in a moonpool is an important problem in the design and operation of various vessels. In this paper, improvements in the modeling of viscous flow effects of the free-surface simulation package ComFLOW are proposed. The improved modeling enables the simulation of events in which detailed viscous flow effects and free-surface motion are strongly coupled, such as the sloshing in a moonpool.

Attention will be given to the discretization of the convective term and the modeling of turbulence. The proposed stabilized central discretization of the convective term shows clear improvements over upwind schemes. State-of-the-art turbulence models, based on the physically relevant invariants of the rate-of-strain tensor, are proposed to model the interaction between resolved and subgrid scales.

The results of these improvements will be assessed for a moonpool sloshing test case.

1 INTRODUCTION

In offshore applications, details of viscous flow effects can become relevant in a variety of circumstances, e.g. when wave run-up on semi-submersible structures or the free-surface motion in a moonpool are concerned. The CFD simulation package ComFLOW has thus far concerned itself mostly with extreme wave impact, so the accurate modeling of viscous flow effects has not yet been a matter of concern. This motivates a novel approach for efficiently simulating viscous flow effects at high Reynolds numbers with the CFD simulation tool ComFLOW.

In ComFLOW, the Navier–Stokes equations can be solved for one-phase and for two-phase flow. The equations are discretized second-order in space, and second-order in time. An improved Volume-of-Fluid (IVOF) algorithm is used for free-surface displacement

[2, 6], which yields an accurate and robust algorithm. The latter property is important in violent flow cases.

Accurate modeling of viscous flow effects in high Reynolds number flows, requires two things. First, a turbulence model should be formulated and implemented that provides accurate results on coarse grids. Secondly, in regions of interest, a high local grid resolution should be achieved in a computationally efficient manner.

The focus of this paper is to assess the performance of improved viscous flow modeling for a practical offshore problem: simulation of the free-surface water motion in a moonpool. For more information on the subject, see [1] and the references therein. In [1], an older version of ComFLOW, which did not contain the detailed modeling of viscous flow effects, has been used to compute the water motion in a moonpool.

In the first section, the discretization of the Navier-Stokes equations is described, followed by an exposition of the turbulence models that have been implemented in ComFLOW. Finally, the performance of the improved viscous flow modeling in ComFLOW for simulating free-surface water motion in a moonpool is investigated.

2 DISCRETIZATION OF THE NAVIER–STOKES EQUATIONS

An excellent model for incompressible (turbulent) fluid flow is provided by the Navier-Stokes equations. The continuity equation

$$\mathcal{M}\mathbf{u} = 0, \tag{1}$$

where $\mathcal{M} = \nabla\cdot$ is the divergence operator, describes conservation of mass. Conservation of momentum is given by

$$\frac{\partial \mathbf{u}}{\partial t} + \mathcal{C}(\mathbf{u},\mathbf{u}) + \mathcal{G}p - \nu\,\mathcal{D}\mathbf{u} = \mathbf{f}, \tag{2}$$

based on the convection operator $\mathcal{C}(\mathbf{u},\mathbf{v}) = \mathbf{u}\cdot\nabla\mathbf{v}$, the pressure gradient operator $\mathcal{G} = \nabla$, the diffusion operator $\mathcal{D}(\mathbf{u}) = \nabla\cdot\nabla\mathbf{u}$ and forcing term $\mathbf{f}$. The kinematic viscosity is denoted by ν.

2.1 Finite-Volume Discretization

The second-order finite-volume discretization of the continuity equation (1) at the 'new' time level $n+1$ is given by

$$M\mathbf{u}_h^{n+1} = -M^\Gamma\mathbf{u}_h^{n+1}, \tag{3}$$

where M acts on the internal of the domain and M^Γ acts on the boundaries of the domain.

Regarding the discretized momentum equation, convection and diffusion term are discretized explicitly in time. The discrete diffusion operator is denoted by D, while $C(\mathbf{u}_h)$ denotes the discrete convection operator. The pressure gradient is discretized at the new time level. In this exposition the forward Euler time integration will be used. Taking the

diagonal matrix Ω to denote the matrix containing the volumes of the control volumes, gives the discretized momentum equation as

$$\Omega \frac{\mathbf{u}_h^{n+1} - \mathbf{u}_h^n}{\Delta t} = -C(\mathbf{u}_h^n)\mathbf{u}_h^n + D\mathbf{u}_h^n - G\mathbf{p}_h^{n+1} - \mathbf{f}. \tag{4}$$

The discrete convection operator is skew-symmetric, i.e.

$$C(\mathbf{u}_h^n) + C(\mathbf{u}_h^n)^* = 0. \tag{5}$$

To make the discretization symmetry-preserving, the discrete gradient operator and the divergence operator are each other's negative transpose, i.e. $G = -M^*$, thus mimicking analytic symmetry $(\nabla\cdot) = (-\nabla)^*$, as in [9].

The solution of this equation is split in two steps. The auxiliary variable $\mathbf{R}_h$ is defined through the equation

$$\Omega \frac{\mathbf{R}_h - \mathbf{u}_h^n}{\Delta t} = -C(\mathbf{u}_h^n)\mathbf{u}_h^n + D\mathbf{u}_h^n - \mathbf{f}. \tag{6}$$

Imposing discrete mass conservation (3) on the new time level $(n+1)$ results in a linear system for the pressure:

$$\Delta t \; M \, \Omega^{-1} \, G\mathbf{p}_h^{n+1} = M\mathbf{R}_h + M^{\Gamma}\mathbf{u}_h^{n+1}. \tag{7}$$

This equation is often referred to as the discrete pressure Poisson equation, as it can be regarded to be a discretization of the equation $\mathcal{M}\mathcal{G}\mathbf{p}_h = \mathcal{M}\mathbf{u}_h$. Note, that here the separate parts $\mathcal{M}$ and $\mathcal{G}$, rather than the the composed operator $\mathcal{M}\mathcal{G}$ are being discretized here.

2.2 Stability of the Spatial Discretization

The symmetry-preserving spatial discretization of the Navier–Stokes equations outlined above assumes a second-order central discretization of the convective term. However, if the (mesh-)Reynolds number of the flow is large, the central discretization can become unstable and show point-to-point oscillations when large gradients or (geometrical) singularities are present in the flow. Typically, the central discretization is stabilized by adding artificial diffusion to the central scheme, resulting in a first-order or second-order upwind discretization.

The damping that is introduced by the artificial diffusion in upwind methods dissipates the energy of scales of motion that can still be represented on the computational grid. Rather than resorting to an excessively dissipative upwind scheme, a slightly modified version of the stabilization procedure proposed by Shyy *et al.* [4] has been implemented. The stabilization procedure consists of a post-processing filter operation acting on the momentum velocities. In these steps, linear momentum is redistributed if point-to-point extrema are detected in the velocity field. The filter is constructed such that it conserves linear momentum.

3 LARGE EDDY SIMULATION MODELS

In order to simulate the high Reynolds number turbulent flows that are associated to offshore applications, large eddy simulation (LES) modeling is necessary. Simply put, the aim of LES is to simulate those scales of motion that can be represented on the computational grid as accurately as possible through modeling of the interaction between resolved and subgrid scales.

In a turbulent flow, the production of small scales takes place through the non-linear convective term. The only mechanism that counteracts the production of small scales of motion is diffusion. The equilibrium between production (by convection) and dissipation (by diffusion) of small scales cannot be reached on the computational grid. This consideration gives rise to two modeling options: either restrict the production of subgrid scales or increase the dissipation of subgrid scales.

3.1 Invariants of the rate-of-strain tensor

Important information of the physics of turbulent flows is contained in the invariants of the rate of strain tensor $S(\mathbf{u}) = \frac{1}{2}\left((\nabla\mathbf{u})^T + \nabla\mathbf{u}\right)$. As is shown in [8], the rate of dissipation of the scales contained in a domain Ω_Δ of size Δ, can be expressed in terms of the second invariant $q(\mathbf{u})$ of $S(\mathbf{u})$ as

$$Q(\mathbf{u}) \equiv \int_{\Omega_\Delta} q(\mathbf{u})\, \mathrm{d}\Omega \equiv \int_{\Omega_\Delta} \frac{1}{2}\mathrm{tr}\; S^2(\mathbf{u})\, \mathrm{d}\Omega. \tag{8}$$

The third invariant, denoted by $r(\mathbf{u})$ can be integrated over the same domain to give

$$R(\mathbf{u}) \equiv \int_{\Omega_\Delta} r(\mathbf{u})\, \mathrm{d}\Omega \equiv \int_{\Omega_\Delta} -\frac{1}{3}\mathrm{tr}\; S^3(\mathbf{u})\, \mathrm{d}\Omega = \int_{\Omega_\Delta} -\det S(\mathbf{u})\, \mathrm{d}\Omega. \tag{9}$$

When positive, the quantity (9) gives a measure for the convective production of scales $< \Delta$. If negative, energy is transferred from subgrid-scale structures to the resolved scales. In order to separate the scales properly, a turbulence model should close the transfer of energy in either direction.

3.2 QR eddy-viscosity model

The analysis in [8] shows that in order to arrive at an appropriate eddy-viscosity model, we evaluate the eddy-viscosity in terms of the invariants as

$$\nu_{\mathrm{eddy}} = \frac{3}{2}\frac{1}{\lambda_\Delta}\frac{|R(\mathbf{u})|}{Q(\mathbf{u})}, \tag{10}$$

where λ_Δ is the eigenvalue of the discrete diffusive operator corresponding to the scale Δ. Taking Δ identical to the grid size, this eigenvalue is a measure for the dissipation of the smallest *resolvable* scales. We will refer to this model as the QR model.

Note that the classical Smagorinsky turbulence model (see e.g. [3]) is formulated in terms of the invariant Q only, and dissipates energy also on well-resolved (even laminar) scales in the flow.

3.3 Regularization Modeling

In order not to interfere with the subtle energetic balance between the convection and diffusion in a turbulent flow on resolved scales, it is important to preserve the symmetries of the Navier-Stokes equations on a discrete level [9]. A symmetry-preserving regularization of the convective term smooths the original convective term while preserving its skew-symmetry. The smoothing takes place through a filter operation $\mathbf{u}_h \mapsto \overline{\mathbf{u}_h}$.

Verstappen [7] applies the filter to the convective term, which yields a family of symmetry-preserving regularization models. The discrete convective term is denoted by $C(\mathbf{u}_h)\cdot\mathbf{u}_h$. The second-order (in terms of the filter length) accurate regularization model from this family is given by

$$C_2(\mathbf{u}_h,\mathbf{u}_h) = \overline{C(\overline{\mathbf{u}_h})\cdot\overline{\mathbf{u}_h}}. \tag{11}$$

Selfadjointness of the filter ensures the skew-symmetry of the original convective term.

The length scale over which the filter smooths the signal will depend on the local flow physics. The analysis in [5] shows that an expression for damping of the convective production of structures beyond length scale Δ can be derived. The damping factor, that we will denote by f_2, is a functional of the (local) filter length α, i.e. $f_2 = f_2(\alpha(\mathbf{u}))$. Balancing the convective production of subgrid scales and the natural diffusive dissipation gives

$$f_2(\alpha)\,\frac{|R(\mathbf{u})|}{Q(\mathbf{u})} = \nu|\lambda_\Delta|, \tag{12}$$

from which the filter length can be determined. The relation with (10) is evident.

3.4 A blended model

Another model that we discern is the blended model, in which both the QR eddy viscosity model and the regularization model play a role, depending on the physics of the flow. The transfer of energy from resolved to subgrid scales (i.e. (9) is positive) is modeled by the QR eddy-viscosity model. The backscatter of energy from subgrid scales to resolved scales (i.e. (9) is negative) is prevented by the regularization model.

The mixture of these models allows for a complete separation of resolved and subgrid scales. Only if the energy is transferred to smaller scales of motion, the kinetic energy is dissipated from the resolved flow structures. The model is closed for backscatter by the regularization of the nonlinear convective interaction between subgrid and resolved scales.

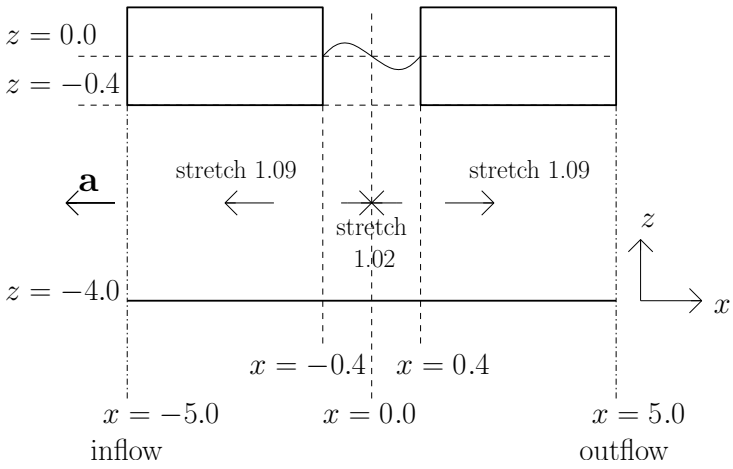

Figure 1: Simulation domain for the moonpool simulations. At the moonpool walls and at the (initial) free-surface position, the grid spacing in x and z direction is 0.01 m., indicated by the dashed line. The grid is stretched with a factor 1.09 towards the inflow and outflow boundaries and towards the bottom of the domain. The grid enclosed by the moonpool edges and the free-surface is slightly stretched (with a factor of 1.02) towards the center of the moonpool.

3.5 The turbulent boundary layer

From a computational point of view it is highly undesirable to refine the grid to the level at which the boundary layer can be resolved. In order to account for the influence of the turbulent boundary layer on the effective wall-shear stress that the outer flow experiences, the Werner-Wengle model is applied [10].

4 SIMULATION OF MOONPOOL WATER MOTION

The simulation of free-surface dynamics in moonpools is an example of an application where possibly violent free-surface motion is coupled to viscous flow details. A realistic simulation of free-surface motion is strongly dependent on the correct prediction of the vortex formation in the moonpool. The combination of coarse grids and upwind discretization techniques dissipate the perturbations that lead to the characteristic roll-up of the shear layer, thus preventing vortex formation at the edges of the moonpool.

In order to illustrate the performance of the stabilized central discretization, the first results of the simulation of water motion in a moonpool (in calm water) will be presented. In the simulations, the moonpool and the computational grid that is fixed to the moonpool geometry are accelerated to a constant speed.

4.1 Setup

In order to model moonpool dynamics in calm water (i.e. in the absence of waves) not the entire ship will be modeled. Instead, the moonpool is modeled as in figure 1. The domain has dimensions (in m.) $[-5.0, 6.0] \times [-0.5, 0.5] \times [-4.0, 0.5]$, and the stretched grid has dimensions $228 \times 10 \times 184$. As the setup of the problem is two-dimensional and most variation is expected to take place in the x-z plane, we hope that 10 uniformly spaced grid points in the are y direction are enough to capture the essential physics. The smallest grid spacing is 0.01 m. and the grid lines to which this spacing applies are indicated by the dashed lines in figure 1.

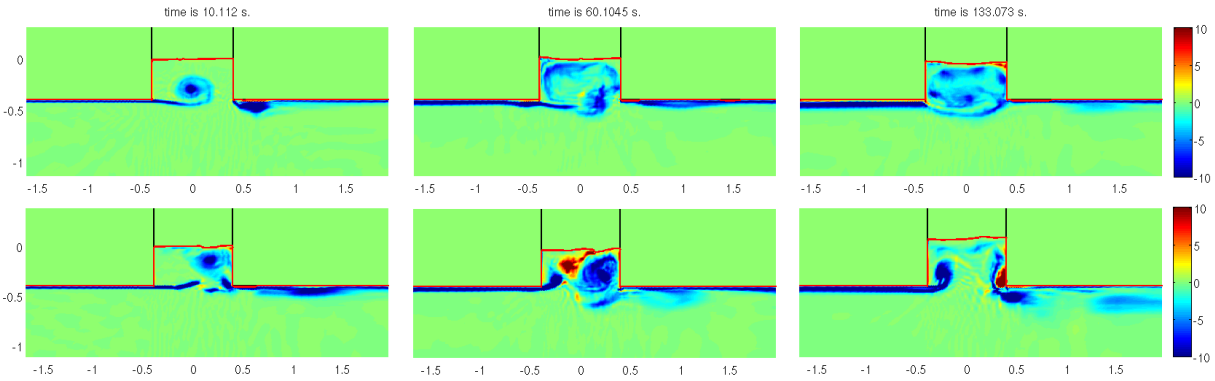

Figure 2: Development of vorticity in time (*from left to right:* 10 s, 60 s, and 133 s) for a final speed (after acceleration) of 0.7 m/s (*top*) and 1.0 m/s (*down*).

In rest, the flat free-surface ($z = 0$) is elevated 0.4 m. above the submerged bottom of the object, i.e. the *draft* is taken to be 0.4 m. The width of the moonpool is 0.8 m. in stream-wise (x) direction and 1.0 m. in cross-stream (y) direction.

Rather than moving the moonpool through the grid or to prescribe the inflow velocity, the moonpool and the grid fixed to the geometry are accelerated from rest. The acceleration is modeled through the forcing term in the Navier-Stokes equations. No-slip boundary conditions are applied at all the moonpool walls.

4.2 Results and discussion

The setup described above is able to capture the essential features of the water motion in the moonpool. Three stages of water motion in the moonpool are illustrated by the vorticity plots that are shown in figure 2. The moonpool is accelerated to two constant speeds: 0.7 m/s and 1.0 m/s.

In the first stage, during acceleration of the moonpool a big vortex is formed at the edge and shear layer roll-up is observed. The vortex travels upward in the moonpool and impinges on the free surface. For the lower speed (0.7 m/s) the vortices that are formed at the edge circulate through the moonpool, deforming the free-surface and inducing a small-amplitude oscillation of the water column (the piston mode).

For the higher speed (1.0 m/s), the elevation of the free-surface is more dramatic, which can clearly be seen from the oscillation of the water height in figure 3. The synchronization of vortex formation and the oscillation of the water column lead to resonant (piston mode) motion of water in moonpool. Moreover, a bore formed by the impinging vortex on the right-side wall of the moonpool is observed to travel back and forth between the right and left wall.

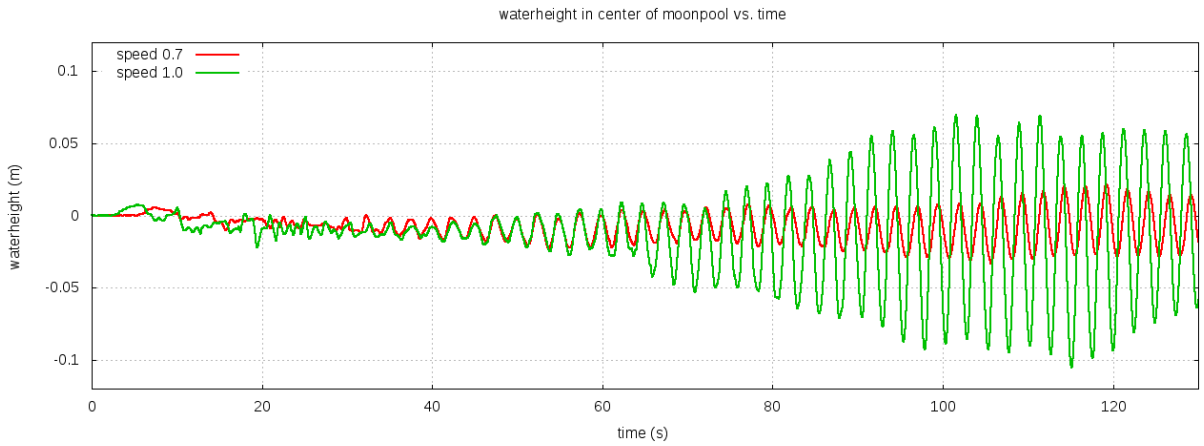

Figure 3: Water height as a function of time for the two final speeds (after acceleration). At a time of about 63 s, the water motion in the moonpool of speed 1.0 m/s resonance behavior is observed.

5 CONCLUSIONS

The free-surface water motion in a moonpool has been simulated with improved viscous flow modeling in ComFLOW. In order to simulate detailed viscous flow effects, it is necessary to employ a symmetry-preserving second-order central discretization of the convective term. As the central discretization is unstable in regions with high velocity gradients, the term is stabilized through the removal of the point-to-point oscillation that might appear around the large gradients. Simulations of the moonpool with the stabilized discrete convective term show that ComFLOW is able to simulate some essential features of water motion in the moonpool. The results are a clear improvement of the first-order (B2) and second-order (B3) upwind discretization which result in a steady state solution, with a stationary recirculation zone present in the moonpool (see the discussion in [1]).

These promising first results ask for a study of the behavior of the solution of the moonpool simulation upon grid refinement and upon the use of different turbulence models that have been described in this paper. A comparison with experimental data will also be possible in the near future.

Finally, the simulation of moonpool water dynamics in the presence of waves will be a subject of study in the near future.

REFERENCES

[1] Gaillarde G. and A. Cotteleer. Water motion in moonpools empirical and theoretical approach. Technical report, Maritime Research Institute Netherlands (MARIN), HMC Heerema, 2005.

[2] K.M.T. Kleefsman, G. Fekken, A.E.P. Veldman, B. Iwanowski, and B. Buchner. A volume-of-fluid based simulation method for wave impact problems. *Journal of Computational Physics*, 206(1):363–393, 2005.

[3] P. Sagaut. *Large Eddy Simulation for Incompressible Flows*. Springer–Verlag, 2001.

[4] W. Shyy, M.-H. Chen, R. Mittal, and H.S. Udaykumar. On the suppression of numerical oscillations using a non-linear filter. *Journal of Computational Physics*, 102(1):49 – 62, 1992.

[5] F.X. Trias and R.W.C.P. Verstappen. On the construction of discrete filters for symmetry-preserving regularization models. *Computers & Fluids*, 40(1):139 – 148, 2011.

[6] A.E.P. Veldman, R. Luppes, T. Bunnik, R.H.M. Huijsmans, B. Duz, B. Iwanowski, R. Wemmenhove, M.J.A. Borsboom, P.R. Wellens, H.J.L. van der Heiden, and P. van der Plas. Extreme wave impact on offshore platforms and coastal constructions. In *30th Conf. on Ocean, Offshore and Arctic Eng. OMAE2011*, Rotterdam, The Netherlands, June 19-24, 2011 (paper OMAE2011-49488).

[7] R.W.C.P. Verstappen. On restraining the production of small scales of motion in a turbulent channel flow. *Computers & Fluids*, 37(7):887–897, 2008.

[8] R.W.C.P. Verstappen. When does eddy viscosity damp subfilter scales sufficiently? *Journal of Scientific Computing*, 49(1):94–110, 2011.

[9] R.W.C.P. Verstappen and A.E.P Veldman. Symmetry-preserving discretization of turbulent flow. *Computers & Fluids*, 187:343–368, 2003.

[10] H. Werner and H. Wengle. Large-eddy simulation of turbulent flow over and around a cube in a plate channel. In *8th Symposium on Turbulent Shear Flows*, pages 155–168. Springer–Verlag, 1991.